T-tubule Disruption Promotes Calcium Alternans in Failing Ventricular Myocytes: Mechanistic Insights from Computational Modeling

Michael Nivala, Zhen Song, James N. Weiss, Zhilin Qu

Supplemental Information

To validate the generality of our conclusions, we used an alternative ventricular myocyte model developed by Restrepo et al [1] with a detailed spatiotemporal Ca cycling system to simulate some of the key results in this study. Compared to the model (see Nivala et al [2]) in the current study which uses the RyR formulation by Stern et al [3], the model developed by Restrepo et al uses a different RyR model which lacks the cytosolic Ca-dependent inactivation of RyR but incorporates instead SR luminal Ca regulation of RyR through Ca-calsequestrin binding. The myocyte model by Restrepo et al also has a lower spatial resolution compared to Nivala et al, and is thus computationally faster. The formulations of other ionic currents are similar in the two models, since both were based on the action potential model developed by Mahajan et al [4].

Using the ventricular myocyte model by Restrepo et al., we first repeated simulations in Fig.3, and obtained the results shown in Fig.S1. Whether the Ca channel conductance was reduced by 30% (panel A), 30% of LCC clusters were removed from the cell (panel B), or 30% LCC clusters were removed with the corresponding

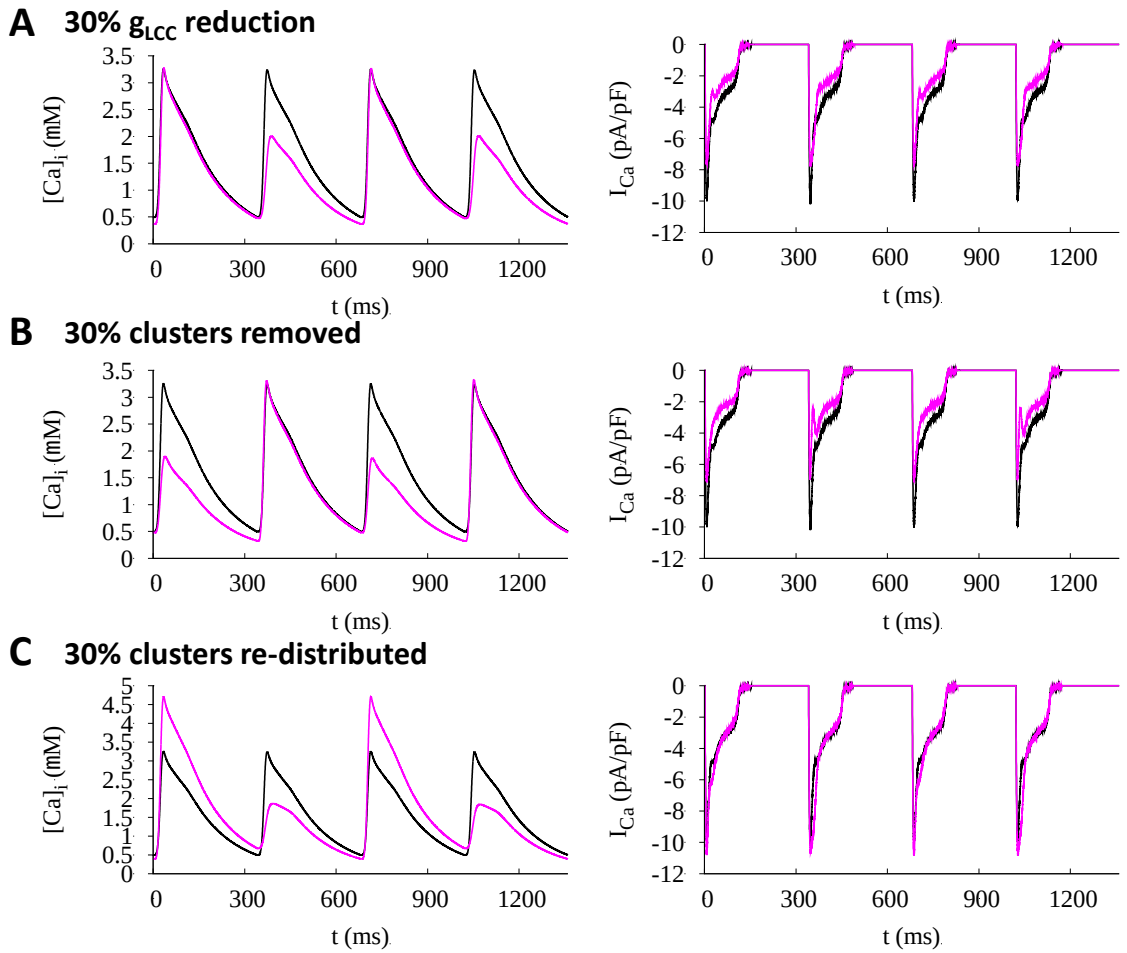

Fig.S1.Ca alternans induced by reduction of Ca channel conductance (A), removal of LCC clusters (B), and re-distribution of the LCCs (C). Black traces show control and the purple traces correspond to the altered Ca channel conductance or distribution.

LCCs re-distributed into the sub-membrane space (panel C), alternans occurred under all three conditions, agreeing with the results in Fig.3. The difference are that the morphologies of the Ca transient and $I_{Ca,L}$ are not identical to those shown in Fig.3. The pacing cycle length was also different (PCL=340 ms in Fig.S1 and PCL=500 ms in Fig.3). Note that after re-distribution of the LCCs to the sub-membrane space, the inactivation of the Ca current became slower as expected (compare the purple trace with the black trace in panel C of Fig.S1). Next, we carried out simulations comparing the onset of Ca alternans by showing bifurcation diagrams that plot the peak $[Ca]_i$ against PCL for normal SERCA (panel A in Fig.S2) and 50% reduction of maximum SERCA activity (Panel B in Fig.S2) under the condition in which 30% of LCC were re-distributed. After SERCA downregulation, the onset of the Ca alternans occurred PCL=1,100 ms (panel B) instead of PCL=360 ms (panel A). This agrees well with the observations shown in the man text using the model by Nivala et al. If we reduced the SERCA to the same extent for the other two cases and also the control case shown in Fig.3, the PCL at the onset of Ca alternans exhibited roughly the same changes (i.e., onset of alternans changed from the range of PCL~300 ms to the range of PCL~1.1 sec).

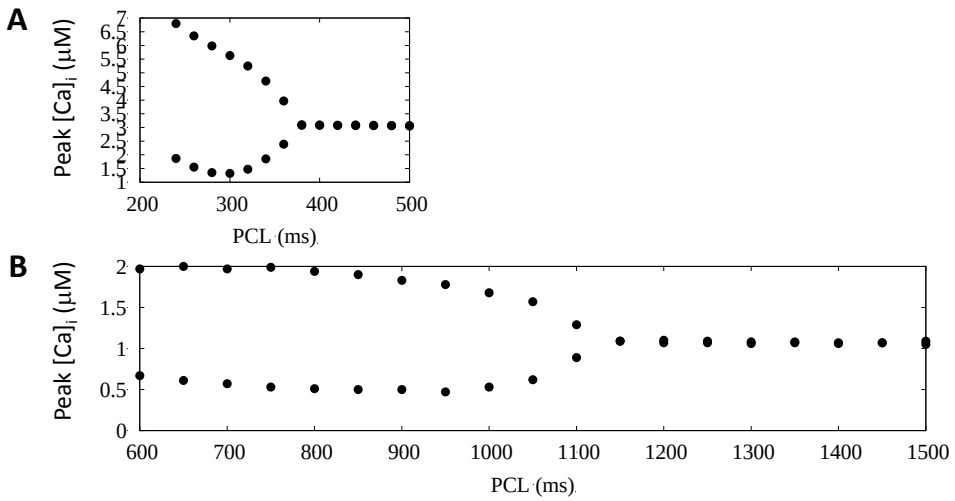

Fig.S2. Bifurcation diagram for normal SERCA (A) and 50% reduction of maximum SERCA (B). Other conditions are the same as in panel C in Fig.S1.

References:
[1] Restrepo JG, Weiss JN, Karma A. Calsequestrin-mediated mechanism for cellular calcium transient alternans. Biophys J. 2008;95:3767-89.
[2] Nivala M, de Lange E, Rovetti R, Qu Z. Computational modeling and numerical methods for spatiotemporal calcium cycling in ventricular myocytes. Front Physiol. 2012;3:114.
[3] Stern MD, Pizarro G, Rios E. Local control model of excitation-contraction coupling in skeletal muscle. J Gen Physiol. 1997;110:415-40.
[4] Mahajan A, Shiferaw Y, Sato D, Baher A, Olcese R, Xie L-H, et al. A rabbit ventricular action potential model replicating cardiac dynamics at rapid heart rates. Biophys J. 2008;94:392-410.